

Iridium–Bismuth Cluster Complexes Yield Bimetallic Nano-Catalysts for the Direct Oxidation of 3-Picoline to Niacin

Richard D. Adams,^{*,†} Mingwei Chen,[†] Gaya Elpitiya,[†] Matthew E. Potter,[‡] and Robert Raja^{*,‡}

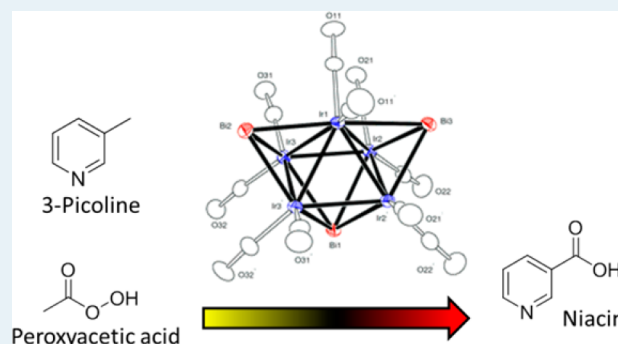
[†]Department of Chemistry and Biochemistry, University of South Carolina, Columbia, South Carolina, 29208, United States

[‡]School of Chemistry, University of Southampton, Highfield, Southampton SO17 1BJ, U.K.

S Supporting Information

ABSTRACT: The reaction of $\text{Ir}_3(\text{CO})_9(\mu_3\text{-Bi})$, **1**, with BiPh_3 has yielded an iridium–bismuth cluster complex $\text{Ir}_5(\text{CO})_{10}(\mu_3\text{-Bi})_2(\mu_4\text{-Bi})$, **2**. The first examples of bimetallic iridium–bismuth nanoparticles have been subsequently synthesized from **1** and **2**, and these have been securely anchored onto the inner walls of mesoporous silica. These isolated, bimetallic iridium–bismuth nanoparticles display a superior catalytic performance, when compared to their analogous monometallic counterparts and equivalent physical mixtures, in the C–H activation of 3-picoline to yield niacin.

KEYWORDS: nanocluster, selective oxidation, iridium–bismuth, niacin, catalytic synergy, anchored nanoparticles, C–H activation



Probing the origins of the catalytic synergy between multimetallic active centers in porous solids, wherein a Platinum Group Metal (PGM) such as Ru, Pt, or Rh, is alloyed with suitable oxophiles such as Sn, Bi, or Mo facilitates the rational design of well-isolated, single-site nanoparticle catalysts, that exhibit enhanced stability and improved catalytic performance.^{1,2} Tailoring suitable oxophiles in combination with multimetallic clusters has afforded intrinsic compositional control at the nanoscale, with the added advantage of controlling the morphology, size, and shape of the ensuing naked-metal nanoparticles.^{3–5} Such a design approach could be integrated with custom-made support modifications (e.g., tuning the hydrophobicity) to yield both functional and structural synergies facilitating structure–property relationships to be established.⁶ The precise controlled synthesis of catalytically active metal nanoparticles has been of great interest in recent years,^{7,8} with the ever-expanding target of creating discrete single-sites. With a view to achieving this goal, a number of elegant strategies using inorganic porous supports,^{9–11} polymer-stabilized matrixes,¹² and framework extrusion processes¹³ have been developed. Despite the intrinsic merits of these approaches,^{9–13} the desire to modulate catalytic activity and selectivity at the nanoscale, through the skillful choice of appropriate metal combinations and their concomitant oxophilic analogues, for generating uniform, discrete, well-defined, multifunctional single-sites, remains a challenging prospect.¹⁴

Bismuth on oxide supports has been shown to catalyze the oxidation of certain hydrocarbons heterogeneously.¹⁵ Bismuth molybdate is well-known for its ability to catalyze the ammoxidation of propene.¹⁶ We have recently shown that a

bimetallic rhenium–bismuth catalyst, derived from a rhenium–bismuth complex $\text{Re}_2(\text{CO})_8(\mu\text{-BiPh}_2)_2$, can selectively convert 3-picoline to 3-nicotinonitrile.² The ability of the oxophile (bismuth in this case) to interact favorably with the mesoporous silica support, through the covalent-bond formation between the oxophilic metal and pendant silanol groups, renders this nanoparticle catalyst amenable for oxidation reactions.^{3,5} Furthermore, the capping of the CO ligands on the nanocluster precursor improves the degree of site-isolation, leading to the creation of the catalytically active nanoparticle catalyst. It has been previously demonstrated^{1–5} that the subsequent removal of the CO ligands, generates uniform (<5 nm), well-defined, anchored bimetallic nanoparticles, where the bismuth plays a pivotal role in securing the nanoclusters to the support and ensuring its compositional integrity.^{3–5} Furthermore, it has also been demonstrated that bismuth plays a key role in enhancing the catalytic efficiency in a range of selective oxidation reactions.^{17–19} Most notable is the combination of bismuth with precious metals to form Pd–Bi¹⁷ and Pt–Bi¹⁸ species. While the exact role of bismuth in such catalysts is not conclusive, it has been suggested that the production of 2,5-furandicarboxylic acid (FDCA) from hydroxymethylfurfural (HMF) was appreciably increased owing to the favorable interaction between Bi atoms and π -electrons in the furan ring.¹⁸ There are also other plausibilities attributing the promoter ability of Bi to its oxophilicity,^{6,17} which enhances the ability of bismuth to activate molecular

Received: October 4, 2013

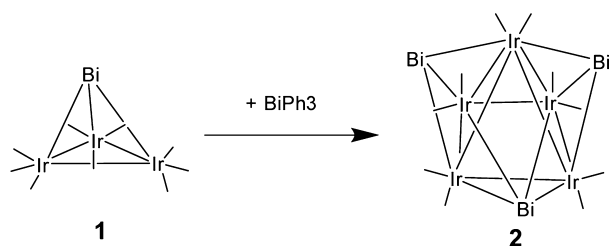
Revised: November 15, 2013

Published: November 18, 2013



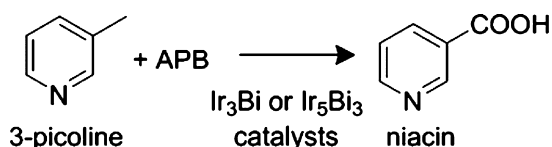
oxygen thereby facilitating α -H abstraction.¹⁹ These unique properties of the bismuth prompted us to devise other bimetallic catalysts, and we report herein, for the first time, the design of two novel iridium–bismuth bimetallic nanoclusters that are derived from new Ir–Bi complexes. Preliminary catalytic studies outlining the performance of these new iridium–bismuth nanoparticle catalysts for the *direct* oxidation of 3-picoline to niacin (Figure 1) are reported, offering a subtle contrast to the previously reported² ammoxidation route to nicotinonitrile (precursor to niacin). Until recently, the only example of an iridium–bismuth complex was the compound $\text{Ir}_3(\text{CO})_9(\mu_3\text{-Bi})$, **1**, that was reported by Schmid et al.²⁰ We have recently prepared a number of iridium–bismuth complexes containing germanium and tin ligands from complex **1** by reactions with HGePh_3 and HSnPh_3 .²¹ We have now found that **1** reacts with BiPh_3 to yield the new higher nuclearity complex $\text{Ir}_5(\text{CO})_{10}(\mu_3\text{-Bi})_2(\mu_4\text{-Bi})$, **2** in high yield (91%), see Scheme 1. Compound **2** was

Scheme 1. Schematic of the Transformation of 1 to 2 by Reaction with BiPh_3 ^a



^aCO ligands are shown only as lines.

characterized crystallographically by single-crystal X-ray diffraction, and an ORTEP diagram of its molecular structure is shown in Figure 2.²² The molecule lies on a reflection plane in the solid state. Compound **2** contains five iridium atoms arranged in the form of a square pyramid.



APB = Acetylperoxyborate

Figure 1. Oxidation of 3-picoline to niacin using APB.

Complex **2** contains three bridging bismuth atoms: atom Bi(1) is a quadruple bridge that spans the base of the Ir_5 square pyramid; the other two, Bi(2) and Bi(3), are triply bridging ligands that bridge oppositely positioned triangular faces of the square pyramid. The Ir–Ir and Ir–Bi bond distances, Ir(1)–Ir(2) = 2.7824(7) Å, Ir(1)–Ir(3) = 2.8226(7) Å, Ir(2)–Ir(3) = 2.7903(7) Å, Ir(2)–Ir(2') = 2.8255(9) Å, Ir(3)–Ir(3') = 2.7796(9) Å, Ir(1)–Bi(3) = 2.8322(9), Ir(1)–Bi(2) = 2.7623(9), Ir(2)–Bi(3) = 2.6868(7), Ir(2)–Bi(1) = 2.8004(7), Ir(3)–Bi(2) = 2.7002(7), Ir(3)–Bi(1) = 2.8185(7) are similar to those found in **1**, (Ir–Ir av = 2.759(2) Å), (Ir–Bi av = 2.734(2) Å).⁷

Initial catalytic studies have revealed that two novel iridium–bismuth catalysts (derived from the Ir_3Bi and Ir_5Bi_3 cluster complexes, see details below) are indeed active for the direct

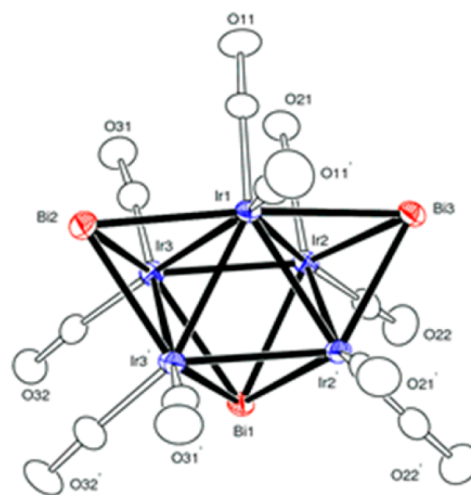


Figure 2. ORTEP diagram of the molecular structure of $\text{Ir}_5(\text{CO})_{10}(\mu_3\text{-Bi})_2(\mu_4\text{-Bi})$, **2** showing 30% thermal ellipsoid probability. Selected interatomic bond distances (Å) and angles (deg) are as follows: Ir(1)–Ir(2) = 2.7824(7), Ir(1)–Ir(3) = 2.8226(7), Ir(2)–Ir(3) = 2.7903(7), Ir(2)–Ir(2') = 2.8255(9), Ir(3)–Ir(3') = 2.7796(9), Ir(1)–Bi(3) = 2.8322(9), Ir(1)–Bi(2) = 2.7623(9), Ir(2)–Bi(3) = 2.6868(7), Ir(2)–Bi(1) = 2.8004(7), Ir(3)–Bi(2) = 2.7002(7), Ir(3)–Bi(1) = 2.8185(7).

oxidation of 3-picoline to niacin (Figure 1).² Niacin is a key component of the NADH/NAD⁺ system that is known to play a key role in many processes related to human metabolism.²³ Also known as vitamin B₃, niacin is an essential food element; deficiencies can lead to the disorder known as Pellagra.²³ Niacin is also known to exhibit benefits for treatments of cholesterol-related problems.²⁴ Therefore the synthesis of niacin is of great interest, as evidenced by the range of industrial processes employed to produce it, by direct oxidation as well as via its precursor, nicotinamide, that is generated by ammoxidation of 3-picoline followed by hydrolysis—see Scheme 3 of reference 2.^{25–27} Industrially viable routes for niacin production are well-established with solid, metal-oxide catalysts yielding over 87 mol % at 300 °C,²⁶ and microbial biocatalysts (*Rhodococcus rhodochrous*) producing nicotinamide in a continuous fashion, albeit in a multistep fashion.²⁷ While our previous work with the Re–Bi catalysts achieve C–H activation of 3-picoline via ammoxidation to achieve low yields (<5 mol %) of niacin using an excess of sacrificial NH_3 ,² we have adopted a more direct oxidative approach, as a proof-of-concept study, with these novel IrBi catalysts for the single-step oxidation of 3-picoline to niacin.

Compounds **1** and **2** were deposited onto mesoporous (MCM-41) silica supports by the incipient wetness method and then both were converted into bimetallic IrBi nanoparticles by thermal treatments under vacuum. They were subsequently evaluated for their ability to oxidize 3-picoline to niacin catalytically by using acetylperoxyborate (APB) as the oxidant. Representative high angle annular dark field (HAADF) high resolution transmission electron microscopy images of the Ir_3Bi and Ir_5Bi_3 nanoparticles after use in catalysis are shown in Figure 3. As can be seen the particles are uniformly dispersed and are less than 2 nm in diameter. It can also be seen that the porous character of the support was maintained during the calcination/particle formation process. Analysis of their compositions by energy dispersive X-ray emission spectroscopy (EDS) are consistent with the Ir_3Bi and Ir_5Bi_3 compositions of

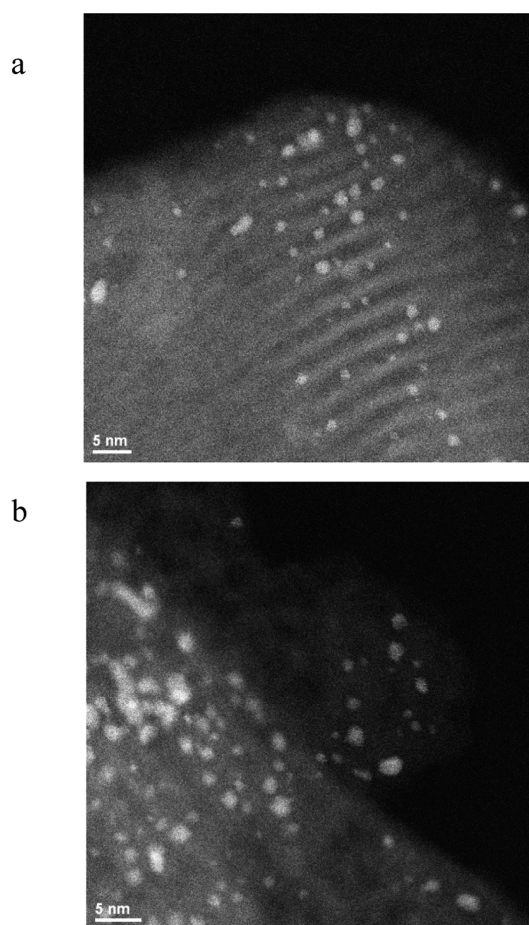


Figure 3. HAADF–HRTEM images of Ir₃Bi (a) and Ir₃Bi₃ (b) nanoparticles on MCM-41 after use in catalysis at 65 °C. The catalysts were preconditioned/activated at 300 °C for 2 h before use.

the precursor complexes, see Supporting Information, Tables S2 and S3.

The Ir₃Bi nanoparticles obtained from **1** were tested for the direct oxidation of 3-picoline to niacin by using the oxidant APB. APB has been shown to be a useful reagent for selective oxidation reactions under mild conditions, serving as a solid source of active oxygen by liberating peroxyacetic acid (PAA) in situ when dissolved in water.²⁸ For comparisons, supported forms of pure Ir and pure Bi, 3Ir/1Bi (created from a solution of a mixture of Ir₄(CO)₁₂ and BiPh₃ combined in the appropriate ratio), Ir₃Bi₃ nanoparticles obtained from compound **2** and 5Ir/3Bi particles (created from a solution of a mixture of Ir₄(CO)₁₂ and BiPh₃ combined in the appropriate ratio) were also tested. The best catalytic results were obtained by preheating the nanoparticles to 300 °C for 2 h under vacuum before use. The catalytic tests were performed at 65 °C for a period of 45 min. The results of the various tests are shown in the chart in Figure 4 where blue represents the conversion of 3-picoline, red represents the selectivity of the conversion to niacin, and purple represents the turnover number (TON) for niacin formation. (See also Supporting Information, Figures S3–S6 for further catalytic details on the nature of the support, the effect of calcination temperature on the reactivity and selectivity along with catalyst recycle studies).

Pure Ir and pure Bi are ineffective catalysts as represented by the very low TONs for Niacin. The principal side product is 3-picoline-N-oxide, **3**, which is the major product of oxidation

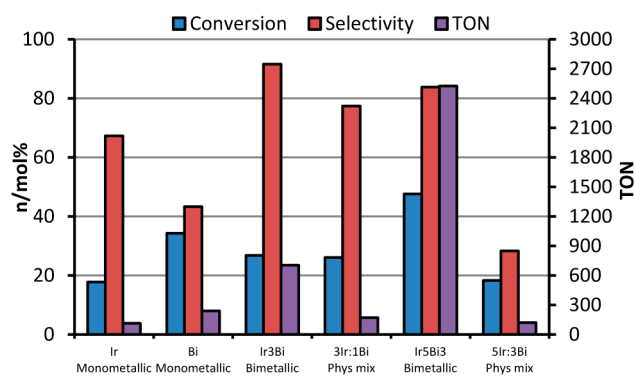


Figure 4. Comparisons of catalytic behavior of the monometallic and bimetallic Ir and Bi catalysts on MCM-41. The experiments with the physical mixtures further highlight the merits of the bimetallic cluster-based analogues. Reaction conditions: 15 mmol of 3-picoline, 3:1 molar ratio of picoline:peroxyacetic acid (yielded from APB), 25 mL of H₂O, 150 mg of catalyst, 3.5 mmol of monoglyme internal standard, 65 °C, 45 min.

with pure Bi on the support. The contrasting catalytic behaviors and catalytic opportunities afforded through the utilization of bimetallic nanoclusters are outlined in Figure 5. The

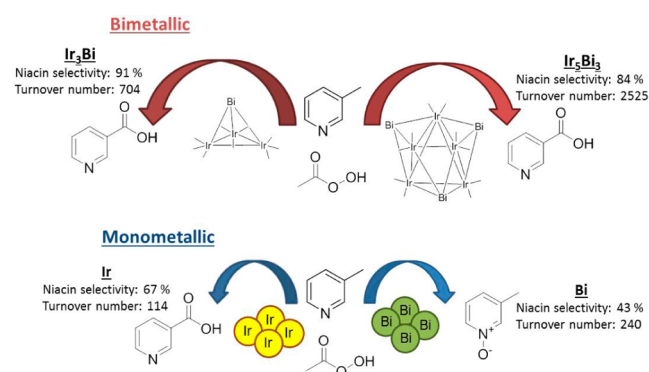


Figure 5. Schematic representation of the contrasting catalytic behaviors afforded by the Ir/Bi containing catalysts.

monometallic Ir and Bi catalysts display distinctly different catalytic profiles (see also Supporting Information, Figures S7–S10 for kinetic profiles); while Ir clearly shows an increased selectivity for niacin, it is far less active than its Bi counterpart, which has a greater propensity for the formation of picoline N-oxide. This difference in activity suggests that the monometallic Ir catalysts facilitate a targeted reaction pathway necessary to form niacin from picoline; whereas the monometallic Bi catalysts is far more proficient in activating the oxidant, which evokes a more diverse range of oxidation products.

The bimetallic catalysts derived from **1** and **2** are superior to the bimetallics derived by coimpregnation (the physical mix), and they exhibit the best selectivity and TONs for niacin.

The attributes of the two individual metal centers are maximized by combining them to generate intimately mixed bimetallic IrBi nanoclusters, which display vastly enhanced selectivity toward the desired niacin along with a concomitant increase in catalytic efficiency (TON). The differing behavior of the 3Ir:1Bi and Ir₃Bi catalysts (the former being a physical mixture prepared using identical moles of monometallic Ir and Bi) strongly suggests that a specific structural integrity of the cluster is fundamental in optimizing the overall selectivity and

efficiency of the catalysts in the oxidation reaction. Through careful synthetic design of the bimetallic precursor, one can ensure that the Ir and Bi metals are in close proximity to one another; a feature that cannot be readily controlled or guaranteed with the preparation of the bimetallic physical mixture. By using a cluster-based precursor, where the structural and compositional integrity can be controlled at the molecular level, it is possible to exploit the individual benefits of the two metals to facilitate a synergistic enhancement in overall catalytic behavior resulting in significant improvements in catalytic turnover. Thus, the Bi atoms are able to readily activate the oxidant, while the adjacent Ir atoms selectively form the niacin via CH activation processes upon the 3-picoline, ultimately creating an effective spillover catalyst.

The catalyst derived from the Ir₃Bi₃ cluster exhibited the best activity for both conversion and catalytic efficiency (TON). This may be attributed to the Ir/Bi ratio becoming closer to unity, thereby promoting a more efficient transfer of activated intermediates between the two metal sites. As with the Ir₃Bi, the cluster derived Ir₅Bi₃ catalyst was far superior to the analogous physical mixture catalyst (5Ir:3Bi), further highlighting the importance of the structural and compositional integrity provided by the cluster precursor.

In summary, the first higher nuclearity iridium–bismuth cluster complex **2** has been synthesized and structurally characterized. The first examples of bimetallic IrBi nanoparticles have been synthesized from the bimetallic IrBi molecular cluster complexes **1** and **2**. In a proof-of-concept study, these bimetallic nanoparticles exhibit superior catalytic activity for the direct oxidation 3-picoline to niacin, compared to their monometallic analogues. By using cluster-based bimetallic precursors, where the compositional integrity can be better controlled at the molecular level, it is possible to produce superior nanocatalysts to better exploit the benefits of the individual metals by synergistic complementarity in the overall catalytic behavior. It is believed that these new iridium–bismuth catalysts will exhibit superior catalytic activity for other types of hydrocarbon oxidation reactions and will pave the way to an emerging family of precious metal-heavy main group metal bimetallic catalysts.^{2,16,29}

■ ASSOCIATED CONTENT

Supporting Information

Experimental details on catalyst synthesis, crystallographic data collection and analysis, TEM (before and after catalysis) and catalysis protocols. Also included is EDS analysis, and associated catalytic and kinetic results. This material is available free of charge via the Internet at <http://pubs.acs.org>.

■ AUTHOR INFORMATION

Corresponding Authors

*E-mail: Adamsrd@mailbox.sc.edu (R.D.A.).

*E-mail: R.Raja@soton.ac.uk (R.R.).

Notes

The authors declare no competing financial interest.

■ ACKNOWLEDGMENTS

This research was supported by the National Science Foundation CHE-1111496 (R.D.A.). R.R. wishes to thank Honeywell International (U.S.A.) for financial support.

■ REFERENCES

- (1) Hermans, S.; Raja, R.; Thomas, J. M.; Johnson, B. F. G.; Sankar, G.; Gleeson, D. *Angew. Chem., Int. Ed.* **2001**, *40*, 1211–1215.
- (2) Adams, R. D.; Blom, D. A.; Captain, B.; Raja, R.; Thomas, J. M.; Trufan, E. *Langmuir* **2008**, *24*, 9223–9226.
- (3) Adams, R. D.; Boswell, E. M.; Captain, B.; Hungria, A. B.; Midgley, P. A.; Raja, R.; Thomas, J. M. *Angew. Chem., Int. Ed.* **2007**, *46*, 8182–8185.
- (4) Hungria, A. B.; Raja, R.; Adams, R. D.; Captain, B.; Thomas, J. M.; Midgley, P. A.; Golovko, V.; Johnson, B. F. G. *Angew. Chem., Int. Ed.* **2006**, *45*, 4782–4785.
- (5) Thomas, J. M.; Adams, R. D.; Boswell, E. M.; Captain, B.; Grönbeck, H.; Raja, R. *Faraday Discuss.* **2008**, *138*, 301–315.
- (6) Gianotti, E.; Shetti, V. N.; Manzoli, M.; Blaine, J. A. L.; Pearl, W. C., Jr.; Adams, R. D.; Coluccia, S.; Raja, R. *Chem.—Eur. J.* **2010**, *16*, 8202–8209.
- (7) (a) Humphrey, S. M.; Grass, M. E.; Habas, S. E.; Niesz, K.; Somorjai, G. A.; Tilley, T. D. *Nano Lett.* **2007**, *7*, 785–790. (b) Vicente, B. C.; Nelson, R. C.; Singh, J.; Scott, S. L.; van Bokhoven, J. A. *Catal. Today* **2011**, *160*, 137–143. (c) Bal, R.; Tada, M.; Sasaki, T.; Iwasawa, Y. *Angew. Chem., Int. Ed.* **2006**, *45*, 448–452.
- (8) (a) Ide, M. S.; Hao, B.; Neurock, M.; Davis, R. J. *ACS Catal.* **2012**, *2*, 671–683. (b) Lobo-Lapidus, R. J.; McCall, M. J.; Lanuza, M.; Tonnesen, S.; Bare, S. R.; Gates, B. C. *J. Phys. Chem. C* **2008**, *112*, 3383–3391. (c) Boucher, M. B.; Zugic, B.; Cladaras, G.; Kammert, J.; Marcinkowski, M.; Latwon, T. J.; Sykes, E. C. H.; Flytzani-Stephanopoulos, M. *Phys. Chem. Chem. Phys.* **2013**, *15*, 12187–12196.
- (9) Herzog, A. A.; Kiely, C. J.; Carley, A. F.; Landon, P.; Hutchings, G. J. *Science* **2008**, *321*, 1331–1335.
- (10) Ishia, T.; Kinoshita, N.; Okatsu, H.; Akita, T.; Takei, T.; Haruta, M. *Angew. Chem., Int. Ed.* **2008**, *47*, 9265–9268.
- (11) Corma, A.; Serna, P. *Science* **2006**, *313*, 332–334.
- (12) Kesavan, L.; Tiruvalam, R.; Ab Rahim, M. H.; bin Saiman, M. I.; Enache, D. I.; Jenkins, R. L.; Dimitratos, N.; Lopez-Sanchez, J. A.; Taylor, S. H.; Knight, D. W.; Kiely, C. J.; Hutchings, G. J. *Science* **2011**, *331*, 195–199.
- (13) Hinde, C. S.; Van Aswegen, S.; Collins, G.; Holmes, J. D.; Hor, T. S.; Raja, R. *Dalton Trans.* **2013**, *42*, 12600–12605.
- (14) Manzoli, M.; Shetti, V. N.; Blaine, J. A. L.; Zhu, L.; Isrow, D.; Yempally, V.; Captain, B.; Coluccia, S.; Raja, R.; Gianotti, E. *Dalton Trans.* **2012**, *41*, 982–989.
- (15) (a) Dumitriu, D.; Bârjega, R.; Frunza, L.; Macovei, D.; Hu, T.; Xie, Y.; Pârvolescu, V. I.; Kaliaguine, S. *J. Catal.* **2003**, *219*, 337–351. (b) Zhao, J.; Qian, G.; Li, F.; Zhu, J.; Ji, S.; Li, L. *Chin. J. Catal.* **2012**, *33*, 771–776. (c) Qian, G.; Ji, D.; Lu, G.; Zhao, R.; Qi, Y.; Suo, J. *J. Catal.* **2005**, *232*, 378–385.
- (16) Hanna, T. A. *Coord. Chem. Rev.* **2004**, *248*, 429–440.
- (17) Rass, H. A.; Essayem, N.; Besson, M. *Green Chem.* **2013**, *15*, 2240–2251.
- (18) Wenkin, M.; Ruiz, P.; Delmon, B.; Devillers, M. *J. Mol. Catal. A: Chem.* **2002**, *180*, 141–159.
- (19) He, Y.; Wu, Y.; Yi, X.; Weng, W.; Wan, H. *J. Mol. Catal. A: Chem.* **2010**, *331*, 1–6.
- (20) Kruppa, W.; Blaeser, D.; Boese, R.; Schmid, G. *Org. Chem.* **1982**, *37B* (2), 209–213.
- (21) Adams, R. D.; Chen, M.; Elpitiya, G.; Zhang, Q. *Organometallics* **2012**, *31*, 7264–7271.
- (22) Crystallographic Data for **2** are as follow: Crystal System = orthorhombic, Space Group: *Pnma*, *a* = 16.3842(13) Å, *b* = 14.3198(11) Å, *c* = 9.2009(7) Å, $\alpha = \beta = \gamma = 90.00^\circ$, *V* = 2158.7(3) Å³, 1982 reflections, *R* = 0.0286, *R_w* = 0.0830, GOF = 0.99. See Supporting Information for additional details.
- (23) Kirkland, J. B. Niacin. In *Handbook of Vitamins* 4th ed.; Rucker, R., Zempleni, J., Suttie, J. W., McCormick, D. B., Eds.; Taylor and Francis: New York, 2007; pp 191–232.
- (24) (a) Ali, K. M.; Wonnert, A.; Huber, K.; Wojta, J. *Br. J. Pharmacol.* **2012**, *167*, 1177–1194. (b) Grundy, S. M. *Am. J. Cardiol.* **1992**, *70*, 127–132.
- (25) Chuck, R. *Appl. Catal. A* **2005**, *280*, 75–82.

(26) Petzoldt, J.; Wilmer, H.; Rosowski F. WO Patent, WO2005/118, 2005.

(27) Shaw, N. M.; Robins, K. T.; Kiener, A. *Adv. Synth. Catal.* **2003**, *345*, 425–435.

(28) (a) Raja, R.; Thomas, J. M.; Greenhill-Hooper, M.; Doukova, V. *Chem. Commun.* **2007**, 1924–1926. (b) Vishnuvarthan, M.; Paterson, A. J.; Raja, R.; Piovani, A.; Bonino, F.; Gianotti, E.; Berlier, G. *Microporous Mesoporous Mater.* **2011**, *138*, 167–175. (c) Raja, R.; Thomas, J. M.; Xu, M.; Harris, K. D. M.; Greenhill-Hooper, M.; Quill, K. *Chem. Commun.* **2006**, 448–450.

(29) (a) Mallat, T.; Bodnar, Z.; Hug, P.; Baiker, A. *J. Catal.* **1995**, *153*, 131–143. (b) Brandner, A.; Lehnert, K.; Bienholz, L. M.; Claus, P. *Top. Catal.* **2009**, *52*, 278–287. (c) Jang, J. H.; Goddard, W. A., III *Top. Catal.* **2001**, *15*, 273–289. (d) Jang, J. H.; Goddard, W. A., III *J. Phys. Chem. B* **2002**, *106*, 5997–6013. (e) Pudar, S.; Oxgaard, J.; Chenoweth, K.; van Duin, A. C. T.; Goddard, W. A., III *J. Phys. Chem. C* **2007**, *111*, 16405–16415.